JOURNAL OF BACTERIOLOGY, Nov. 1983, p. 888–897
0021-9193/83/110888-10$02.00/0

Vol. 156, No. 2

Initial Stages in the Morphogenesis of Nitrogen-Fixing Stem Nodules of *Sesbania rostrata*

H. C. TSIEN,[1] B. L. DREYFUS,[2] AND E. L. SCHMIDT[1]*

Department of Microbiology, University of Minnesota, Minneapolis, Minnesota 55455,[1] and Laboratoire de Biologie des Sols, ORSTOM/CNRS, Dakar, Senegal[2]

Received 15 April 1983/Accepted 19 August 1983

Morphogenesis of stem nodules in *Sesbania rostrata* was studied over a period of 6 days after inoculation with an appropriate species of *Rhizobium*. Nodulation sites were initially slightly raised, circular areas 0.3 to 0.6 mm in diameter and 4 to 5 mm apart in vertical rows along the length of the stem. Each site was underlaid by an adventitious root primordium. A site became susceptible to infection by a specific *Rhizobium* sp. when the root primordium broke through the epidermis, leaving a fissure. Rhizobia multiplied within this fissure and colonized the exposed intercellular spaces. The infection extended inward as narrow, branched intercellular threads moved into a cortical meristematic zone, where cell division was initiated, and invagination of infection thread branches into adjacent plant cells followed. Rhizobia were released into the plant cells and surrounded immediately by plant membrane. Intracellular rhizobia divided actively, leading to bacteroid-filled cells. Infected areas enlarged and coalesced as the nodule matured.

Nitrogen-fixing nodules of leguminous plants are generally formed on roots and function in soil. However, above-ground nodules have been described in *Neptunia oleraceae* (13) and *Aeschynomene indica* (2, 15), and Dreyfus and Dommergues (7, 8) recently reported on an annual tropical legume, *Sesbania rostrata*, which bears nodules profusely along the stem as well as on the roots. These stem nodules are caused by specific, fast-growing rhizobia and are capable of nitrogen fixation. Apart from its aerial site of nitrogen fixation, the *S. rostrata-Rhizobium* system is of interest in several important respects. Nodulation and nitrogen fixation by the stem nodules are not repressed by available nitrogen in the soil (7), stem nodule fixation capacity is very high, exceeding 250 kg of N_2 fixed per hectare in 52 days (8), and substantial potential for the system as a green manure in rice cultivation has been demonstrated (12).

Nodulation on stems of *S. rostrata* occurs at predetermined locations identified as incipient root sites (10). The sites, designated stem mamillae, consist of a subepidermal dome pierced by an incipient root (10). When infected by specific *Rhizobium* sp., tissue at these sites proliferates into stem nodules. We report here on the details of stem nodule morphogenesis in *S. rostrata*.

MATERIALS AND METHODS

Microorganism and culture. *Rhizobium* species ORS571, which was originally isolated from stem nodules of *S. rostrata* (7), was used. The stock culture was maintained on tryptic soy agar (Difco Laboratories, Detroit, Mich.). Cultures were grown at 26°C with shaking in YL liquid medium (9). A 1-day-old culture which contained about 10^8 cells per ml was used directly for plant inoculation.

Plant culture and inoculation. *S. rostrata* plants were grown in the field (in Dakar, Senegal, in pots containing 2 kg of soil). After 1 month, a sample of inoculated stem was taken as a control, and stems of remaining plants were inoculated with the *Rhizobium* culture by means of a small spray bottle. Nodule samples were taken 24 h after inoculation and daily thereafter through day 6.

Transmission electron microscopy. Nodule samples were fixed in glutaraldehyde (8% in water stored under nitrogen; Polysciences Inc., Warrington, Pa.) solution in cacodylate buffer, 25 mM (pH 7), at a concentration of 2.5% for 2 h. Samples were washed three times with cacodylate buffer, postfixed with 1% osmium tetroxide in cacodylate buffer overnight, and then washed three times with cacodylate buffer. Dehydration, embedding, sectioning, and examination with an electron microscope at 80 kV were done as previously described (14).

Scanning electron microscopy. Fixed samples were dehydrated through graded acetone solution, subjected to critical-point drying, and coated with gold in a Denton evaporator equipped with a rotary tilting attachment. Specimens were examined in a Hitachi-Perkin-Elmer S450-1 scanning electron microscope operated at 20 kV. Scanning electron micrographs were recorded on type 55 Polaroid film.

Measurement of nodule diameter. Fixed nodules or nodulation sites were sliced in half under a dissecting microscope, and the diameter of the specimens was

measured to 0.1 mm. Ten to fifteen nodules were measured at each sampling date. Results are reported as means ± standard deviation.

RESULTS

Stem nodules of *S. rostrata* and the distinctive sites at which they are formed are shown in Fig. 1. Young mature nodules were spherical, 0.3 to 0.8 cm in diameter, and symmetrical or with irregular lobes. Uninfected nodulation sites (Fig. 1, arrowhead) were round, slightly swollen areas 0.3 to 0.6 mm in diameter, spaced 4 to 5 mm apart in vertical rows on the stem. There were three or four such vertical rows spaced evenly around the circumference of the stem.

Uninoculated nodulation site. Mature nodulation sites had an epidermal dome, a root primordium, and a circular fissure (Fig. 2). The root primordium had a bullet-shaped tip and a widened base continuous with the stem cortex. The vascular cylinder of the root primordium is shown with its tip portion fractured away, leaving a conical depression (Fig. 2, double arrowhead). Two regions of small, apparently dividing cells occurred at the base of the root primordium (Fig. 2, arrowhead). These cells form a thin collar of actively dividing tissue and overlie a portion of the large, highly vacuolated cortical cells surrounding the vascular cylinder. This is apparently a meristematic zone. The epidermal dome was made up of cortical cells covered by epidermal cells continuous with the stem epidermis. Rupture of these tissues by the enlarging root primordium left a fissure or annular cavity a few cell diameters wide between the dome and the root. The interior of the fissure was free of bacteria. Root hairs were not observed in the epidermis of the root primordium.

Initiation of nodulation. Inoculation-induced changes in the nodulation site were evident by the second day. The diameter of the nodulation site was slightly increased (Fig. 3), and slight swelling of the dome was apparent. Examination of cross sections of 1- and 2-day inoculated nodulation sites by scaning electron microscopy and transmission electron microscopy revealed only individual rhizobia widely scattered within the fissure. No plant cells infected with rhizobia could be seen, and no changes were observed in either the meristematic zone cells or the large vacuolated cortical cells surrounding the vascular cylinder of the root primordium. The fact that the nodulation site increased in diameter, however, suggests that meristematic activity was already under way, induced from a distance by the developing infection in the fissure.

Small clusters of rhizobia were found in nodules on the third day. Bacterial cells were scattered within the fissure and extended inward through intercellular spaces. Penetration from the fissure to a distance of two or three plant cells via the intercellular spaces is shown in Fig. 4A. The intercellular spaces adjacent to the fissure are shown in cross section in Fig. 5A, with the arrow pointing toward the inner (root tip base) edge of the fissure. The spaces were well filled with bacteria and notably wide at this point, perhaps widened by active rhizobial development within a confined space. The intercellular spaces narrowed within a short distance laterally and appeared funnel shaped in section (Fig. 5B). These narrow extensions, seen in Fig. 5D in cross section, constitute an intercellular infection thread wherein the rhizobia proliferate and spread within the meristematic zone around the base of the root primordium.

The intercellular nature of the infection thread is shown in Fig. 5C. Examination of both sides of a cell wall shows the absence of a bilayered membrane structure on the *Rhizobium* side of the wall and a cytoplasmic membrane-like structure with membrane vesicles on the plant cell

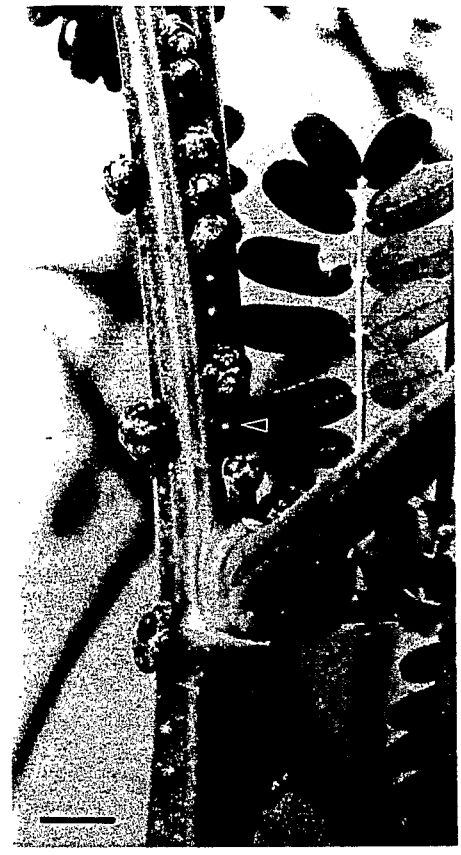

FIG. 1. Nodules and uninfected nodulation sites (arrowhead) on a stem of *S. rostrata*. Mature stem nodules show asymmetrical lobular development. Bar, 1 cm.

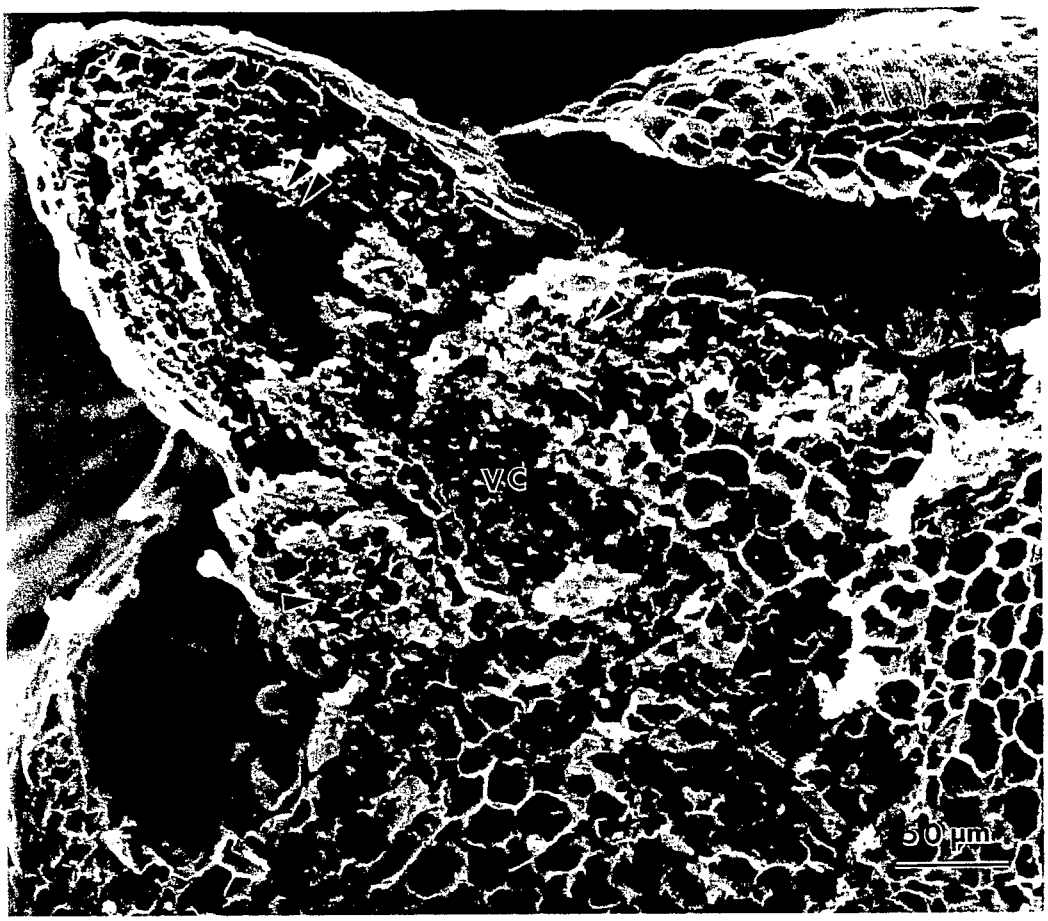

FIG. 2. Scanning electron micrograph of an uninoculated nodulation site sectioned through its center along the stem axis. The uninfected site is composed of a root primordium (center), which pierces the stem cortex and epidermis, leaving a fissure or annular cavity surrounding the root primordium. The vascular cylinder (VC) of the root primordium is shown with the tip portion fractured away, leaving a conical depression (double arrowhead). Single arrowheads indicate a region of small, dense cells on each side of the base of the root primordium.

side of the wall. Intercellular space was usually partially filled with a matrix (Fig. 5D) of moderately electron-dense material assumed to be exopolysaccharide (6); the matrix usually appeared more dense in the vicinity of the plant cell walls.

Infection thread development. Infection thread proliferation into the zone of meristem tissue was evident in 3- and 4-day-old nodules. Nodule size had increased to 0.5 to 1.0 mm in diameter, and rhizobia were relatively abundant within the fissure. Incipient loci of infection (infection centers) were observed in the meristematic zone. These loci first appeared in a low-magnification section as small, dense-appearing regions (Fig. 6A, star).

Within an infective center, infection threads were narrow (one or two rhizobia wide) and well ramified between the cells in the meristematic zone (Fig. 7B). Although infection threads were primarily along cell walls at this stage, there was also evidence of invagination into cells, and some rhizobia were seen free within the plant cells. Invagination into cortical cells as a prelude to intracellular release of rhizobia is shown in Fig. 7A (superimposed arrowhead). The infection threads and their invaginating branches were bound by cell wall (Fig. 7A and B, superimposed arrowheads). Once invaginated into the cytoplasm, the infection thread was surrounded by the plant cytoplasmic membrane (Fig. 7D, arrowhead). Rhizobia already released within the host cell were generally enclosed individually within a membrane (Fig. 7A, arrowhead), although some were seen in the host cell vacuoles (Fig. 7A, double arrowhead) without a surrounding membrane.

Uninfected meristematic zone cells immedi-

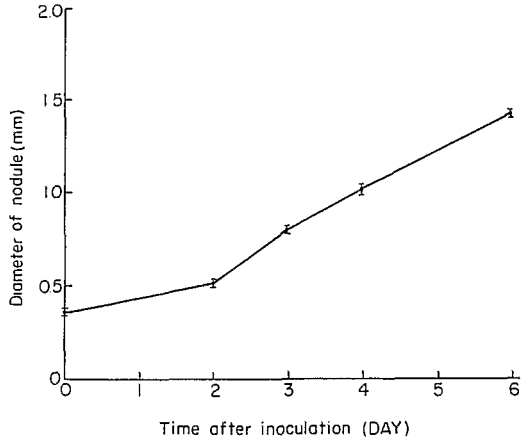

FIG. 3. Increase of nodule size during the first 6 days after inoculation. Vertical bars indicate standard deviations of the measurements of 20 to 30 nodule halves.

ately adjacent to the infective center were small and nearly filled with cytoplasm (Fig. 7C). Cell walls were very thin (Fig. 7C, double arrowhead) suggesting a state of active division, and proplastides were common. A nucleus and densely stained nucleolus were evident in many of the cells. A double-layered nuclear membrane with nuclear pores was clearly visible at higher magnification (micrograph not shown). Cells surrounding the uninfected meristem cells were larger, with thicker walls, large central vacuoles, and proplastides.

Intracellular colonization by rhizobia. Nodule development between days 4 and 6 was characterized by continued enlargement of the nodule, expansion of the infective centers, extensive extracellular proliferation of rhizobia within the fissure, and extensive intracellular colonization of meristematic zone cells by rhizobia. The environment within the fissure was obviously highly favorable to the free-living growth of the specific *Rhizobium* sp., since by the fifth day, the fissure appeared to be virtually filled with rhizobia (Fig. 4B).

At the 5-day stage also, infective centers were clearly expanded and readily recognizable in scanning electron microscopy sections (Fig. 6B, stars). These dense-appearing areas were sometimes of different size, and sometimes only one such area was exposed in cross section. The elongated plant cells comprising infection centers were oriented along their long axes radiating from the center outward (Fig. 8C). The edge of the infective center was marked by a sharp boundary (Fig. 8C, arrowheads) between infected cells and much larger, highly vacuolated cells of the cortex. At high magnification, the cells adjacent to the infective center resembled those

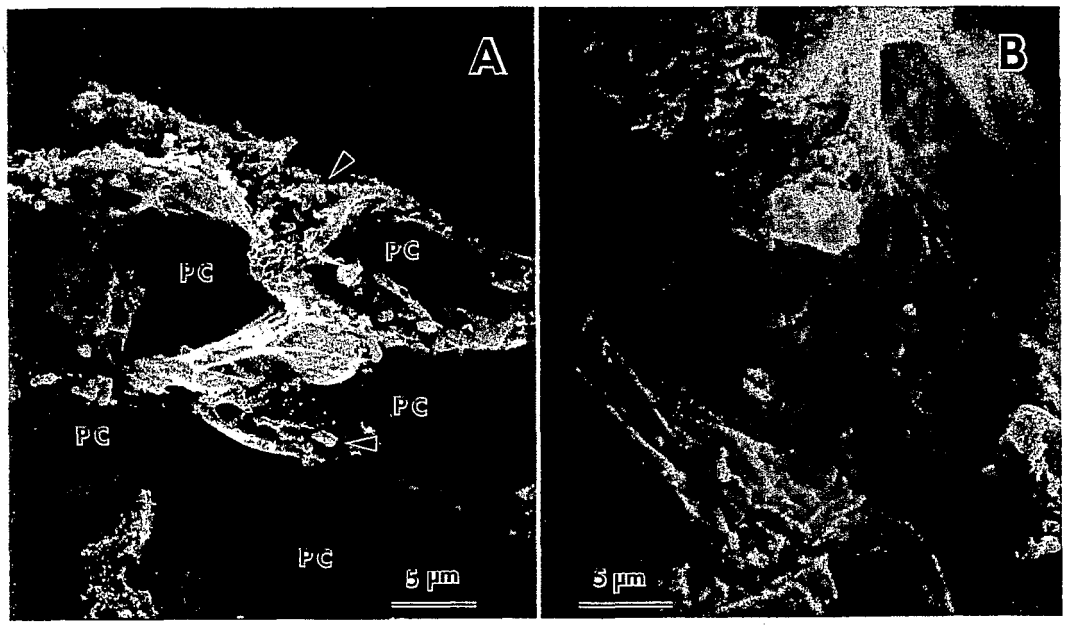

FIG. 4. Scanning electron micrographs of nodule halves showing the area near the edge of the fissure. (A) The inner surface of a 3-day-old nodule. Rhizobia (arrowheads) have penetrated funnel-shaped intercellular spaces between cortical cells to a depth of one or two cells. Plant cells (PC) at the edge of the fissure were highly vacuolated and possibly degenerate. (B) Five-day-old nodule showing proliferation of *Rhizobium* sp. within the fissure.

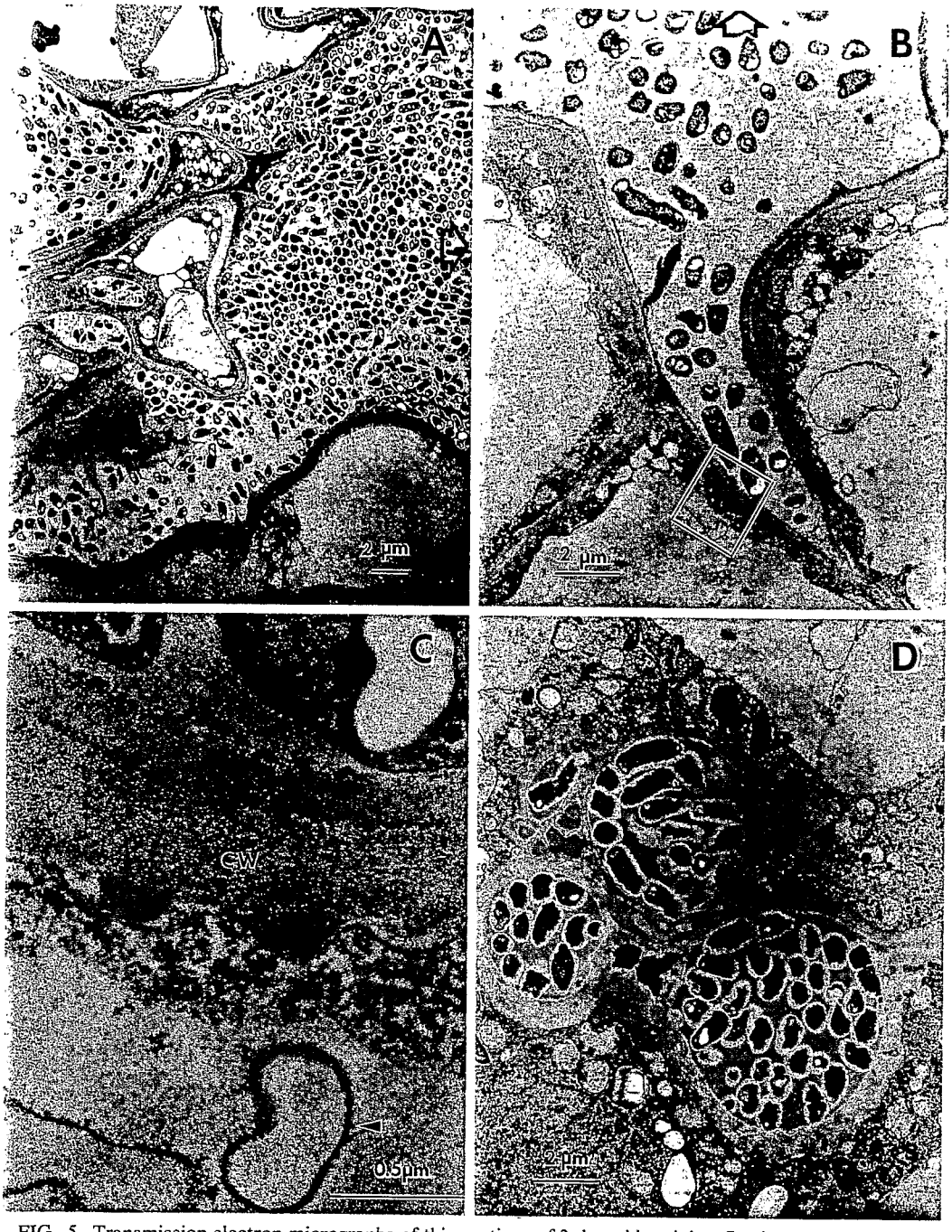

FIG. 5. Transmission electron micrographs of thin sections of 3-day-old nodules. Sections were cut through the edge of the nodules in a plane parallel to the long axis of the root primordium. (A) An intercellular space at the inner edge of the fissure filled with rhizobia. (B) Rhizobia in a funnel-shaped intercellular space leading away from the fissure in the direction of the base of the root primordium. Arrows in (A) and (B) point in the direction of the fissure. (C) Higher magnification of boxed area in (B). Membrane structures (arrowhead) were visible at the plant cell side of the cell wall (CW) but were absent from the *Rhizobium* sp. side. (D) Cross section of three adjacent intercellular spaces filled with rhizobia. Rhizobia within these infection threads were separated from the thread matrix by an electron-transparent zone.

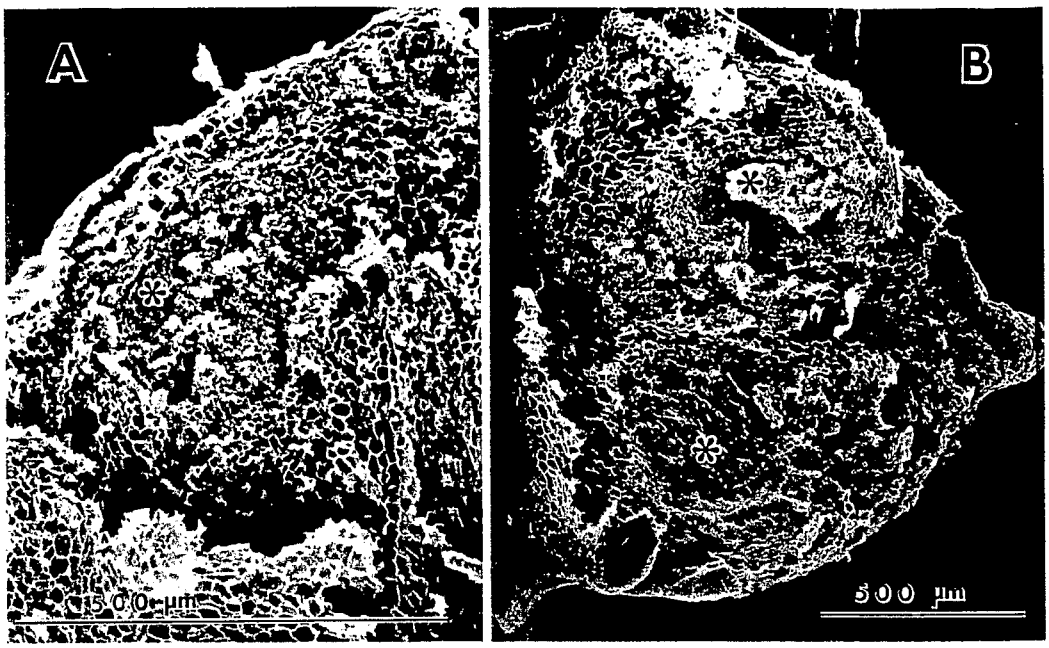

FIG. 6. Scanning electron micrographs of nodules cut through the center parallel to the long axis of the root primordium. (A) A 4-day-old nodule. (B) A 6-day-old nodule. Stars indicate infective centers made up of cells invaded by *Rhizobium* sp.

of the young, 2-day-old nodule and, except for the absence of orderly arrangement, the typical mature and inactive cells found in the center of the vascular cylinder.

The most striking developmental feature of 5- and 6-day nodules was the increased abundance of intracellular rhizobia. Whereas relatively few intracellular rhizobia were seen at 4 days (Fig. 7A), thin section preparations of the infective centers of 6-day nodules showed extensive intracellular colonization (Fig. 8A and B). Rhizobia-filled cells of the same region were also observed by scanning electron microscopy (Fig. 8D). The transition from the intercellular to intracellular state by the rhizobia apparently occurred via breakdown of the infection thread after invagination. Figure 8B shows a tubular infection thread with invaginating intracellular projections. Release of thread matrix (and bacteroids?) is evident on one end (double arrowhead). Bacteroid release is seen more closely in Fig. 7D, where breakdown of an infection thread wall has released thread matrix immediately adjacent to a bacteroid (double arrowhead) already enclosed in a peribacteroid membrane.

Rhizobia released into the host cell cytoplasm were surrounded by a clear zone bounded by a peribacteroid membrane. Peribacteroid membranes can be seen in Fig. 7D and 8B. Rhizobia within the infection thread frequently were surrounded by a clear zone as well, but that zone was never delineated by a membrane (Fig. 7D, superimposed arrowhead). Some rhizobia in the 6-day nodules were dividing within their peribacteroid membranes (Fig. 8A, arrowheads), and many had accumulated poly-β-hydroxybutyrate granules (Fig. 8A and B, white zones within rhizobia). Glycogen and polyphosphate granules (15), the latter frequently associated with fibrous DNA, could be distinguished within the bacteroids at high magnification.

Other general features of the infective center were observed in the 4- to 6-day period. Some uninfected plant cells occurred among surrounding bacteroid-filled cells (Fig. 8A and D). The uninfected cells had one or more central vacuoles and were generally smaller than adjacent infected cells, and frequently their nuclei and sometimes nucleoli (Fig. 8D) were visible. Nodule enlargement was due to enlargement of the infective centers, but there was no evidence of infection thread penetration into the boundary cells. The boundary cells appeared to limit expansion of the infective centers at the lower (deeper) and inner (root base) margins, so that outgrowth was radially outward and upward. Continued enlargement until adjacent infective centers coalesce probably accounts for the larger size and often lobed appearance of the mature nodules.

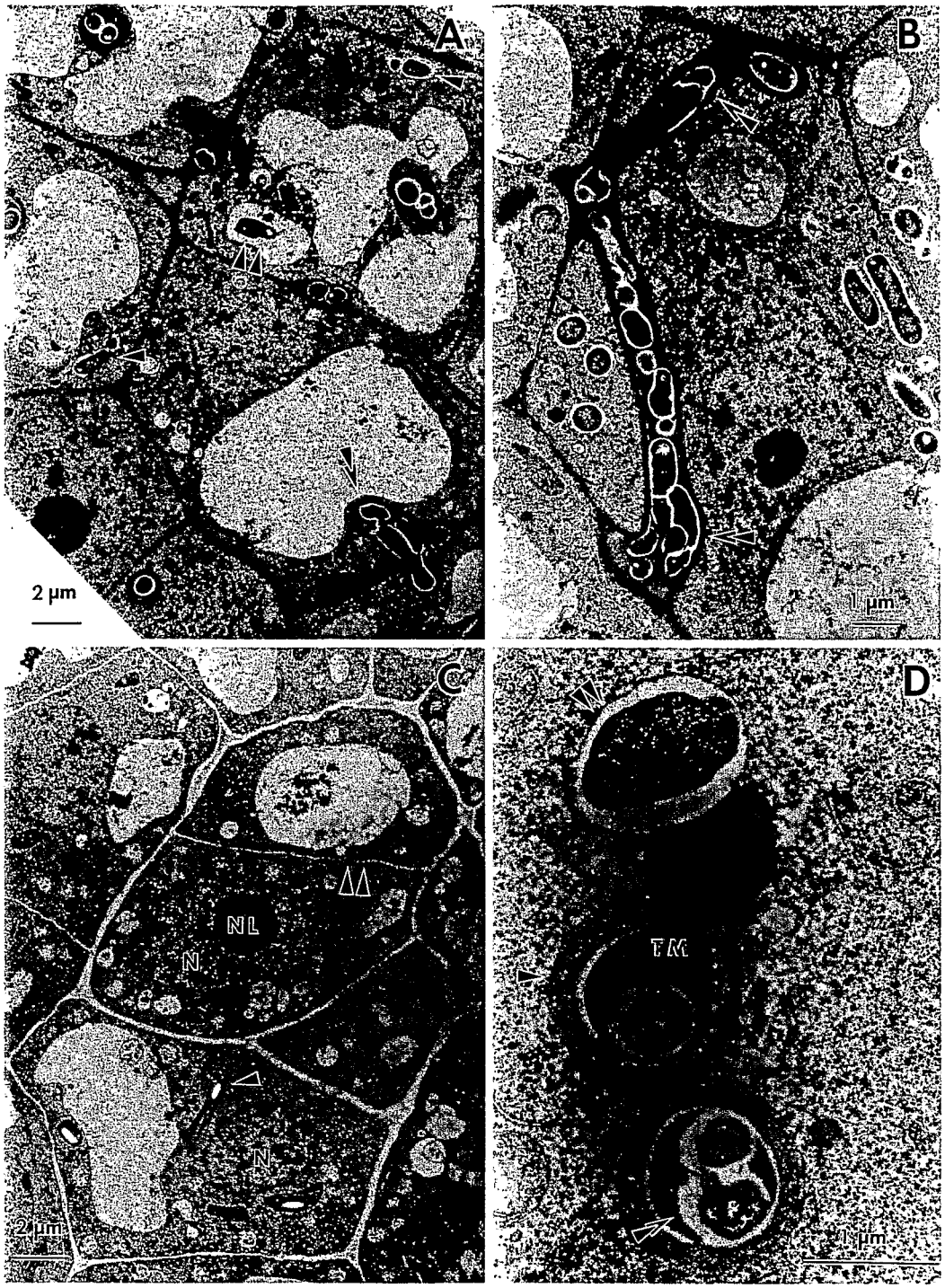

FIG. 7. Thin sections of an infection center in the meristematic zone of 4-day-old nodules. (A) Cortical cells seen at early infection stage with invagination of an infection thread (superimposed arrowhead), membrane-enclosed bacteroids (arrowheads), and a bacteroid without a surrounding membrane (double arrowhead). (B) A long infection thread located intercellularly showing plant cell wall boundary (superimposed arrowhead). (C) Uninfected plant cells within the meristematic zone adjacent to the infected cells seen in (A) and (B). These cells were relatively small and filled with cytoplasm and had a thin cell wall (double arrowhead). The nucleus (N), surrounded by the nuclear membrane and nucleolus (NL), was visible in uninfected cells. Proplastides (arrowhead) were present. (D) Infection thread(s) surrounded by a fibrous wall structurally similar to the plant cell wall. A membrane (arrowhead) was present between host cell cytoplasm and infection thread wall. The clear zones which separated individual rhizobia from the thread matrix were not membrane bound (superimposed arrowhead). A bacteroid is surrounded by a peribacteroid membrane (double arrowhead) and is still in contact with the infection thread matrix (TM) released from the adjacent infection thread.

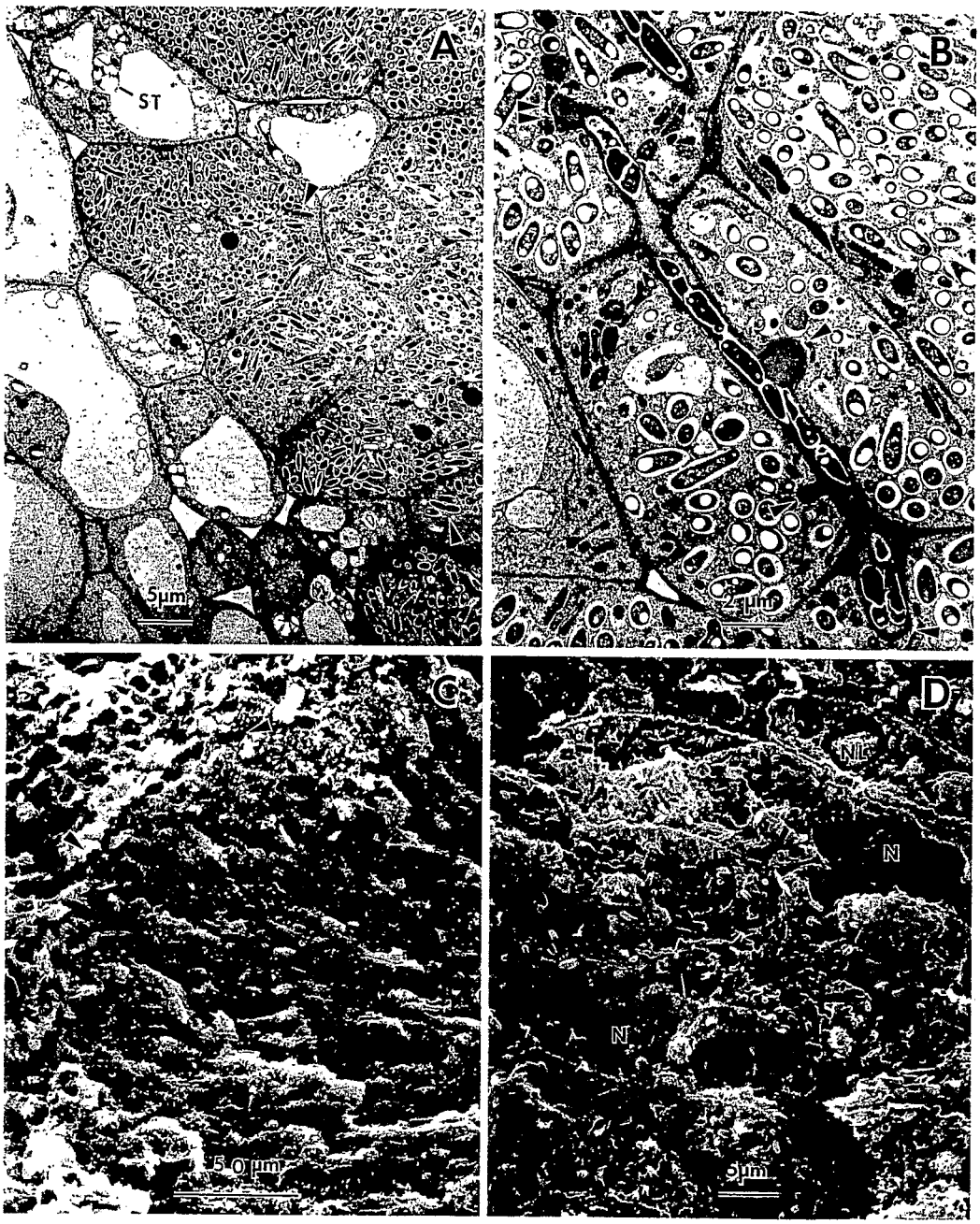

FIG. 8. Infective centers of 5- and 6-day-old nodules. (A) Thin section showing infected and uninfected plant cells at the boundary of an infective center of a 6-day-old nodule. Rhizobia within infected cells were enclosed by plant membranes, and some were dividing (arrowheads). Uninfected cells were generally small, with large central vacuoles and starch granules (ST). Infection threads were not observed in such cells. (B) Infection thread development and invagination seen by thin section of a 6-day-old nodule, penetrating adjacent plant cells (arrowheads). At one end the tip of an invaginating infection thread had dissolved and released thread matrix material into host cytoplasm (double arrowhead). (C) Scanning electron micrograph of the infective center of a 5-day-old nodule. At low magnification infected plant cells were oriented lengthwise radiating from the center of infection (arrow). A sharp boundary (arrowheads) separated two infected and uninfected zones. (D) The same nodule preparation at high magnification shows host cells filled with rhizobia. A few cells were uninfected within the infective center. The nucleus (N) and nucleolus (NL) were visible.

DISCUSSION

The early events in the formation of stem nodules in *S. rostrata* are summarized as follows: (i) colonization of the nodulation site by specific *Rhizobium* sp., (ii) intercellular penetration of rhizobia into the meristematic zone, (iii) establishment by rhizobia of localized infection sites (infective centers) within the meristematic zone, (iv) invagination of intercellular infection threads into cells of the infective center and intracellular release of rhizobia, (v) intracellular growth of rhizobia and bacteroid formation, and (vi) progressive enlargement of infective centers with continued cortical cell division and continued infection thread expansion and invagination. The more unusual aspects of nodule formation in this system include the nature of the nodulation site, the mode of invasion of the rhizobia, and the proliferation of cortical tissues surrounding the incipient adventitious root primordium wherein rhizobial infection begins and within which it expands and spreads.

The stem nodulation site is a beautifully evolved structure capable of initiating either a root system or a nitrogen-fixing system, depending on the environment. The conditions that trigger activation as a nitrogen fixation site are not known, but in view of the natural occurrence of stem nodules only under water-logged soil conditions, it is reasonable to expect that moisture is an important factor. The fissure formed when the root tip breaks through the epidermis of the activated nodulation site provides an excellent microenvironment for inoculant rhizobia. Just how this microenvironment selects for an appropriate *Rhizobium* sp. strain when exposed to natural windborne inoculation is an interesting ecological question. In any case, the specific *Rhizobium* sp. establishes and begins to divide at widely scattered sites on the V-shaped bottom of the fissure. The plant cells exposed at the base and inner face of the fissure are mature, highly vacuolated, nondividing cells with wide intercellular spaces (Fig. 5A). The rhizobia colonize the exposed open spaces and crevices between the cells.

The mode of penetration of rhizobia in the *S. rostrata* stem nodule system is generally similar to that of the peanut, *Arachis hypogaea*, root nodule system. Unlike most root nodules systems, in which the rhizobia enter cortical cells through curled root hair tips by forming an infection thread (3, 6, 11), infection on the peanut root starts by entry into intercellular spaces at the base of root hairs on emerging lateral roots (1, 4, 5). *S. rostrata* stem nodule formation differs from that of the peanut, however, in that the *S. rostrata* nodulation site is without root hairs, and the intracellular penetration in *S. rostrata* is via an infection thread surrounded by a cell wall-like structure. In *A. hypogaea*, penetration into the host cortical cell does not involve a cell wall-bound infection thread (4).

The target area for rhizobia penetrating the root primordium from the fissure is a relatively thin zone of small, dense, cytoplasm-filled cells. This tissue occurs surrounding the base of the root primordium and underlying the base of the fissure by a distance of a few cortical cells (Fig. 2). These cells appear to be cortex derived and highly meristematic (Fig. 7C). Infection spreads within the meristematic zone by extension of intercellular infection threads and into cells in contact with the infection thread.

As in other *Rhizobium*-legume symbioses, the *S. rostrata* stem rhizobia grow profusely within host cells, which become densely packed with bacteroids. The infective centers within the meristematic zone clearly expand and merge as nodules mature at stages later than those examined in this study. It is not clear from our data how the infective zones proliferate, but, if analogous to nodule morphogenesis in root nodules (6, 11), it may be expected that cell division in the meristematic zone is stimulated by the presence of the rhizobia.

ACKNOWLEDGMENT

This research was supported in part by grant DPE-5542-G-SS-3012-00 from the U.S. Agency for International Development.

LITERATURE CITED

1. **Allen, D. N., and E. K. Allen.** 1940. Response of the peanut plant to inoculation with rhizobia with special reference to morphological development of the nodules. Bot. Gaz. (Chicago) **102**:121–142.
2. **Arora, N.** 1954. Morphological development of the root and stem nodules of *Aeschynomene indica* L. Phytomorphology **4**:211–216.
3. **Callaham, D., and J. G. Torrey.** 1981. The structural basis for infection of root hairs of *Trifolium repens* by *Rhizobium*. Can. J. Bot. **59**:1647–1664.
4. **Chandler, M. R.** 1978. Some observations on infection of *Arachis hypogaea* L by *Rhizobium*. J. Exp. Bot. **29**:749–755.
5. **Chandler, M. R., R. A. Date, and R. J. Roughley.** 1982. Infection and root-nodule development in *Stylosanthes* species by *Rhizobium*. J. Exp. Bot. **33**:47–57.
6. **Dart, P.** 1977. Infection and development of leguminous nodules. p. 367–472. *In* R. W. F. Hardy and W. S. Silver (ed.), A treatise on dinitrogen fixation, vol. III. John Wiley & Sons, New York.
7. **Dreyfus, B., and Y. R. Dommergues.** 1980. Non-inhibition de la fixation d'azote atmospherique chez une legumineuse a nodules caulinaires, *Sesbania rostrata*. C.R. Acad. Sci. **291**:767–770.
8. **Dreyfus, B., and Y. R. Dommergues.** 1981. Nitrogen fixing nodules induced by *Rhizobium* on the stem of the tropical legume *Sesbania rostrata*. FEMS Microbiol. Lett. **10**:313–317.
9. **Dreyfus, B. L., G. Elmerich, and Y. R. Dommergues.** 1983. Free-living *Rhizobium* strain able to grow on N_2 as the sole nitrogen source. Appl. Environ. Microbiol. **45**:711–713.
10. **Duhoux, E., and B. Dreyfus.** 1982. Nature des sites d'infection par le *Rhizobium* de la tige de la legumineuse,

Sesbania rostrata Brem. C.R. Acad. Sci. **294**:407–411.
11. **Newcomb, W.** 1981. Nodule morphogenesis and differentiation. Int. Rev. Cytol. **13**(Suppl):247–297.
12. **Rinaudo, G., B. Dreyfus, and Y. R. Dommergues.** 1983. Influence of *Sesbania rostrata* green manure on the nitrogen content of rice crop and soil. Soil Biol. Biochem. **15**:111–113.
13. **Schaede, R.** 1940. Die knollchen der adventiven wasserwurzeln von *Neptunia oleracea* und ihre bakteriensymbiose. Planta **31**:1–21.
14. **Tsien, H. C., and E. L. Schmidt.** 1977. Polarity in the exponential-phase *Rhizobium japonicum* cell. Can. J. Microbiol. **23**:1274–1284.
15. **Yatazawa, M., and S. Yoshida.** 1979. Stem nodules in *Aeschynomene indica* and their capacity of nitrogen fixation. Physiol. Plant. **45**:293–295.